Author/s:
Ranathunga, AS;Perera, MSA;Ranjith, PG;De Silva, GPD

Title:
A macro-scale view of the influence of effective stress on carbon dioxide flow behaviour in coal: an experimental study

Date:
2017-03-01

Citation:
Ranathunga, A. S., Perera, M. S. A., Ranjith, P. G. & De Silva, G. P. D. (2017). A macro-scale view of the influence of effective stress on carbon dioxide flow behaviour in coal: an experimental study. Geomechanics and Geophysics for Geo Energy and Geo Resources, 3 (1), pp.13-28. https://doi.org/10.1007/s40948-016-0042-2.

Persistent Link:
https://hdl.handle.net/11343/283309

Cover Page

Manuscript Title:

A macro-scale view of the influence of effective stress on carbon dioxide flow behaviour in coal: An experimental study

Authors' names:

A.S. Ranathunga[1], M.S.A. Perera[1,2*], P.G. Ranjith[1] and G.P.D. De Silva[1]

[1]Deep Earth Energy Laboratory, Department of Civil Engineering, Monash University, Building 60, Melbourne, Victoria, 3800, Australia.

[2] Department of Infrastructure Engineering, The University of Melbourne, Building 176, Melbourne, Victoria, 3010, Australia.

Corresponding author:

Dr Mandadige Samintha Anne Perera

Department of Infrastructure Engineering,

The University of Melbourne,

Building 176, Melbourne, Victoria,

3010, Australia.

Phone : Phone: +61-3-9035 8649

Fax: +61-3-9035 8649

E-mail: samintha.perera@unimelb.edu.au

Abstract

Existing studies highlight the uncertainty in the process of CO_2 sequestration in deep coal seams, mainly due to the associated CO_2 adsorption-induced coal matrix rearrangements. This complexity is further increased by the highly heterogeneous nature of the coal mass which causes issues in reproducing field conditions under laboratory conditions. The main objective of this study is therefore to determine the permeability behaviour in coal for CO_2 flow using macro-scale reconstituted coal specimens (203 mm in diameter and 1000 mm in length), particularly under various effective stress conditions. A series of core flooding experiments was conducted on Australian brown coal, using an advanced core flooding apparatus, for a range of CO_2 injection pressures and axial stresses. According to the findings, CO_2 permeability decreases with increasing CO_2 injection pressure, and the reduction is greater for super-critical CO_2 at greater depths. The critical zone of influence for CO_2 injection into a selected coal seam is greater at lower injection pressures and at shallow depths, and it reduces with increasing CO_2 pressure and seam depth. CO_2 storage capacity in a selected coal seam is greater at lower depths and higher CO_2 injection pressures. However, the reduction of CO_2 storage capacity with depth was not very significant, which is important for field CO_2 sequestration projects, which normally use deep seams to store CO_2.

Keywords: CO_2 storage; Coal permeability; Core flooding test; Effective stress; Low rank coal

1. Introduction

Due to the capability of reducing the amount of anthropogenic carbon dioxide (CO_2) in the environment, CO_2 sequestration in deep un-mineable coal seams has been identified as an effective method to address global warming (Jing et al. 2015; Verma and Sirvaiya 2016; White et al. 2005). Based on the fact that coal mass has higher affinity to CO_2 than other gases like methane (CH_4) and nitrogen (N_2) due to its greater chemical and physical interaction, the sequestration process in return releases the coal bed methane (CBM), which is an environmentally-friendly energy source with higher efficiency (White et al. 2005). However, according to the research literature (Day et al. 2008; Hol and Spiers 2012; Jing et al. 2015; Larsen et al. 1997; Pan and Connell 2007; Wang et al. 2013), the sequestration of CO_2 disrupts the stability of the original coal structure with apparent changes in coal matrix swelling, which decreases the CO_2 injectability into the coal seam and affects its long-term stability. It is therefore important to study the principles of coal mass swelling and to have a better understanding of the factors affecting this process.

A number of studies have been conducted on coal seam permeability upon CO_2 sequestration and the effects of various factors on this have been highlighted, including injecting CO_2 properties (Jasinge 2010; Day et al. 2008; Pan and Connell 2007; Perera et al. 2011; Siriwardane et al. 2009; Vishal and Singh 2015) and coal mass properties (Merkel et al. 2015; Wang et al. 2013). According to the research, potential coal seams for CO_2 sequestration with higher temperatures and pressures have limited CO_2 flow ability, because CO_2 is in its super-critical state (beyond 7.38 MPa pressure and 31.8^0C temperature CO_2 exists as super-critical fluid) and has higher sorption capacity in such seams.

On the other hand, it is well known that coal is a highly heterogeneous material and it is therefore quite difficult to validate the results obtained from natural coal samples for in-situ coal seams (De Silva 2013). Jasinge (2010) and Liu et al. (2016) found that reconstituted coal (RC) samples with reproducible properties can be used to successfully represent natural coal specimens,

to overcome such difficulties. The following section focuses on some previous studies conducted on RC and natural samples.

1.1 Comparison of fluid flow behaviour in reconstituted and natural coal

To date, many studies have been conducted to identify the flow behaviour in natural coal seams using reconstituted coal samples and satisfactory results have been obtained. Fig. 1 illustrates a study that compares N_2 and CO_2 permeability and related swelling in natural and reconstituted Australian low rank coal (Jasinge, 2010).

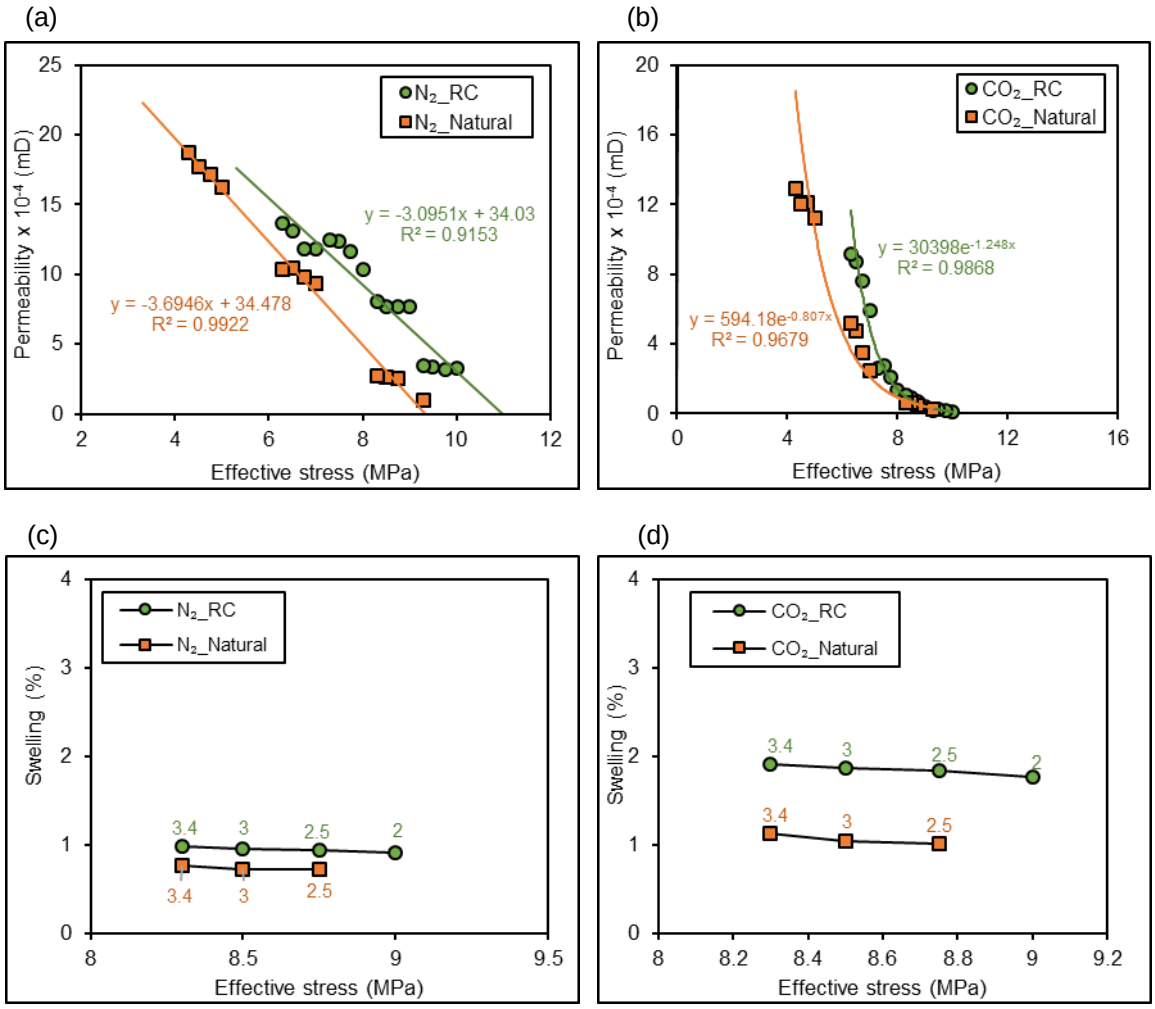

Fig. 1 (a) N_2 and (b) CO_2 permeability variation with effective stress and the variation of coal mass swelling with (c) N_2 and (d) CO_2 flow for reconstituted coal (RC) and natural coal specimens (Jasinge 2010) (The data labels in (c) and (d) denote the respective injection pressures)

According to Fig. 1(a), N_2 flow linearly reduces with increasing effective stress in both natural and RC samples and CO_2 flow (see Fig. 1(b)) follows a negative exponential variation, exhibiting an unfavourable effect of CO_2 exposure to coal permeability. Further, the RC specimens show a higher permeability compared to the natural specimens for both N_2 and CO_2 flow (see Figs. 1(a) and (b)). Similar results were obtained by Liu et al. (2016) who injected CH_4 (~0.69 MPa) to coking coal (from Hexi coal mine, China) at different confining pressures (from around 2-7 MPa) which exhibited higher permeability for RC specimens than natural coal samples. This indicates the difference of fracture system characteristic such as fracture porosity and connectivity of the reconstituted coal sample and the natural coal sample. Further attention to coal mass swelling with N_2 and CO_2 permeation reveals that N_2 injection does not show any significant variation in swelling with effective stress (see Fig. 1(c)) for both natural and RC samples. Conversely, CO_2 flow causes the coal mass swelling to undergo an increasing trend with the increase of injection pressure (see Fig. 1(d)) for both natural and RC specimens. However, RC specimens display a comparatively higher coal matrix swelling compared to natural specimens during CO_2 flow. This is probably caused by the higher amount of CO_2 molecules enter to the coal mass (due to the higher permeability in RC samples compared to natural samples) which will interact with coal mass and create greater swelling. This may also contribute for the observed permeability variations (see Fig. 1(b)) having lower permeability reductions for natural samples than RC samples during CO_2 permeation. However, the correlation between swelling and permeability of coal generally shows a similarity in both natural and RC specimens, allowing the use of RC specimens for experimental purposes (Jasinge 2010, Liu et al. 2016).

1.2 Studies on CO_2 flow behaviour using macro-scale coal specimens

As recorded in the literature (Day et al. 2008; Jasinge 2010; Pan et al. 2010; Perera et al. 2011; Siriwardane et al. 2009; Sun et al. 2016; Vishal and Singh 2015), most coal CO_2 injection studies have been conducted using meso-scale samples (up to around 100 mm in length). This has caused difficulties in confirming the applicability of adsorption theories at a higher scale to the estimation

of CO_2 storage capacity (De Silva 2013). Hence, De Silva (2013) conducted some advanced core-flooding tests using 1 m long and 203 mm diameter (macro-scale) RC low rank coal samples to effectively estimate the CO_2 flow behaviour in coal to overcome the scale effect. De Silva (2013) basically focused on the sub-critical CO_2 flow in large coal samples and Ranathunga et al. (2015) extended this study to super-critical CO_2 to represent actual CO_2 flow behaviour in deep coal seams, considering the CO_2 flow behaviour along the sample. The following sections summarise some major findings of the macro-scale core flooding experiments conducted on CO_2 injection.

- *Sub-critical CO_2 injection*

De Silva (2013) conducted a series of tests of sub-critical CO_2 injection (from 0.4 MPa to 7.4 MPa) under 1, 2, 4, 6 and 8 MPa axial stresses and observed a reduction in CO_2 permeability with increasing CO_2 injection pressure and axial stress (Fig. 2). CO_2 adsorption-induced coal matrix swelling is the main causative fact for this permeability reduction and this was proved by the related swelling data (Fig. 2). According to Fig. 2, the coal volumetric strain is increased with increasing injection pressure. Further, according to the figure, the increase of axial stress causes a reduction in permeability for CO_2 movement, probably due to the greater effective stresses applying on the coal mass.

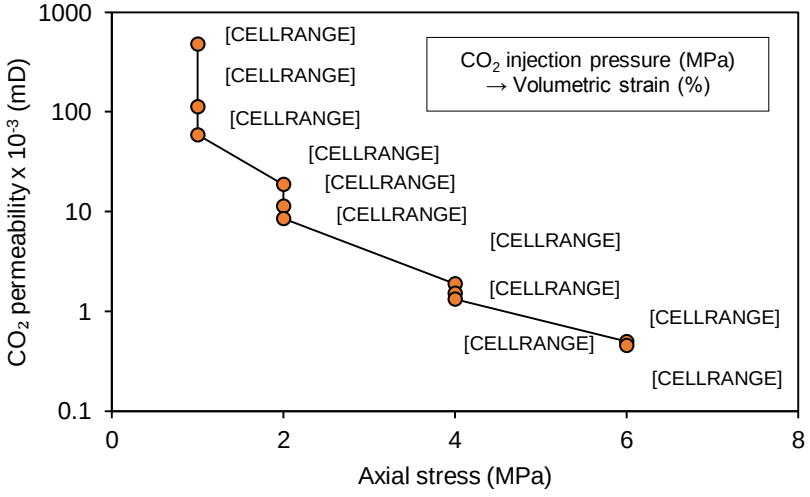

Fig 2. CO_2 permeability variation with the axial stress and volumetric strain for different CO_2 injection pressures (The first value of the label denotes the CO_2 injection pressure (MPa) and the second value denotes the respective volumetric strain (%)) (De Silva 2013)

➢ *Super-critical CO_2 injection*

As potential coal seams for CO_2 sequestration undergo super-critical CO_2 injection, Ranathunga et al. (2015) conducted a series of tests using super-critical CO_2 to understand the variations of CO_2 phase in large-scale coal specimens. They injected 6 to 10 MPa CO_2 into low rank RC specimens under constant 38 ℃ temperature (> 31.8 ℃, the critical temperature of CO_2) and under 11 MPa axial stress. They injected N_2 before (first N_2 injection) and after the CO_2 injection (second N_2 injection) to quantify the CO_2 flow-induced coal mass changes and the N_2 and CO_2 permeability variations obtained are illustrated in Fig. 3.

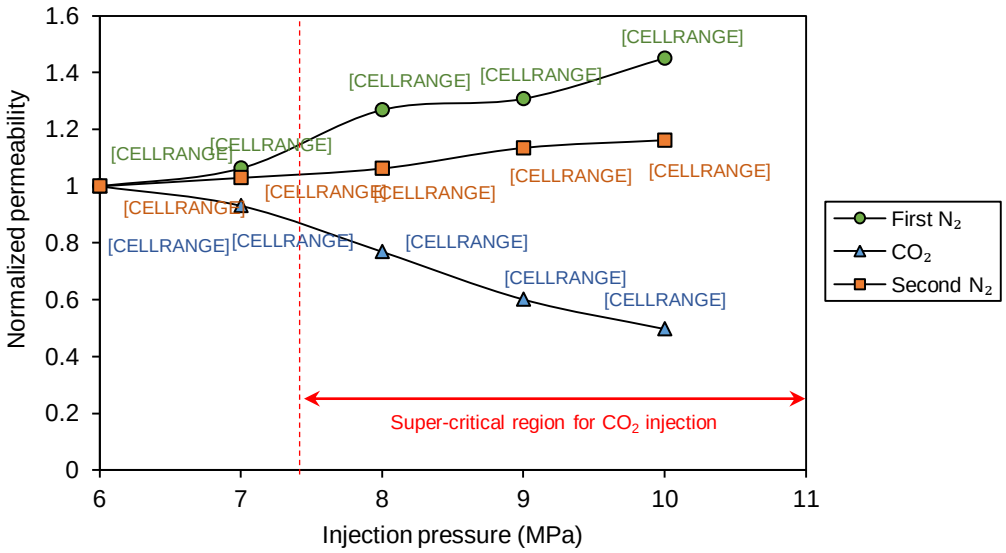

Fig 3. Permeability variation with different injection pressures for first N_2 injection, CO_2 injection and second N_2 injection (Ranathunga et al. 2015) (The data labels indicate the coal specimen's volumetric strain (%) under each injection condition. The permeability values have been normalized by dividing each value by the permeability obtained for 6 MPa in each injection condition)

According to Fig. 3, the results are consistent with the results obtained by De Silva (2013) for sub-critical CO_2, showing a reduction of permeability with increasing CO_2 injection pressure.

140 However, it can be noted that the reduction is comparatively higher in the super-critical region
141 compared to sub-critical CO_2. For example, there is around a 7% decrease in permeability from 6 to
142 7 MPa sub-critical CO_2 injection and around 21% permeability decrease from 8 to 9 MPa super-
143 critical CO_2 injection. This reduction is three times higher than in sub-critical CO_2 flow. The main
144 reason for this observation is the higher adsorption capacity of super-critical CO_2, as a result of its
145 greater chemically active nature, liquid-like density and viscosity that cause greater coal mass
146 swelling compared to sub-critical CO_2 (Day et al. 2008). This is further evident from the volumetric
147 swelling data for both regions (see Fig. 3). Furthermore, the comparative reduction of the second N_2
148 flow compared to the first N_2 flow clearly illustrates the coal mass changes which occur upon
149 exposure to CO_2. For example, at 6 MPa, the first N_2 to the second N_2 injection shows around 17%
150 permeability reduction, and that for 8 MPa is around 31%. As N_2 is a comparatively less adsorptive
151 gas compared to CO_2 (Perera et al. 2011), this observed flow variation clearly occurs due to coal
152 mass swelling during CO_2 flux.

153 In addition, De Silva (2013) observed a decrease in CO_2 permeability in coal with increasing
154 effective stress (axial stress) for sub-critical CO_2. Hence, it is important to investigate how super-
155 critical CO_2 flow changes with increasing effective stress. Ranathunga et al. (2016) conducted a
156 series of meso-scale experiments to investigate this super-critical CO_2 effect for similar low rank
157 natural coal samples and observed the similar behaviour of CO_2 flow and permeability reduction
158 with increasing effective stress. Table 1, lists some of the results obtained by Ranathunga et al.
159 (2016) for 6 to 7 MPa (sub-critical CO_2), 7 to 8 MPa (the CO_2 phase changing region), and 8 to 9
160 MPa (super-critical CO_2) flow increments under 11, 14 and 17 MPa axial stresses.

161 According to Table 1, reduction of permeability with increasing effective stress is evident
162 and greater permeability reduction in deep coal seams is shown during CO_2 sequestration.
163 Furthermore, this reduction is gradually increased when the CO_2 phase is changed, being
164 comparatively greater in super-critical CO_2 compared to sub-critical CO_2. The opportunity for more
165 adsorptive super-critical CO_2 molecules to interact with the coal matrix, creating increased matrix

rearrangements is the main reason for this observation (Perera et al. 2011). However, this may create complications for CO_2-ECBM in deeper coal seams for CO_2 injectability and productivity. Hence, further research is needed on this to gain better understanding of this phenomenon for application in the field.

Table 1. Variation of CO_2 permeability with effective stress (Ranathunga et al. 2016)

	Permeability variation (%)		
Confining pressure (MPa)	6 to 7 MPa sub-critical CO_2 flow increment	7 to 8 MPa CO_2 phase changing region	8 to 9 MPa super-critical CO_2 flow increment
11 (around 400m depth)	-1.8*	-9.7*	-19.2*
14 (around 500m depth)	-7.6*	-12.4*	-25.1*
17 (around 600m depth)	-10.6*	-23.2*	-30.3*

*A negative sign indicates the permeability reduction

The main objective of this study is therefore to develop knowledge of coal mass behaviour with CO_2 exposure using macro-scale reconstituted low rank coal samples, particularly to identify the influence of axial stress on large-scale samples. The present study can therefore be considered as an extension of the work of De Silva (2013) and Ranathunga et al. (2015), which pays more attention to super-critical CO_2 flow behaviour in coal located at various depth using macro-scale coal samples. An effort was also made to quantify the corresponding CO_2 storage capacity variation with various effective factors (CO_2 phase, pressure and seam depth).

2 Experimental methodology

The advanced core-flooding apparatus available in the Deep Earth Energy Research Laboratory (DEERL) at Monash University (Fig. 4) was used to conduct this study. A detailed description of the apparatus can be found in De Silva (2013) and the experimental procedure is briefly described below.

2.1 Sample preparation

In this experiment RC samples were prepared using powdered low rank brown coal. The coal powder was obtained from coal blocks taken from the Hazelwood open-cut coal mine at Morwell in

Gippsland, Victoria. The samples had a natural moisture content of around 55%. The RC specimen construction procedure is shown in Fig. 5, and the detailed methodology adopted to construct the RC samples can be found in De Silva (2013) and Ranathunga et al. (2015).

(a)

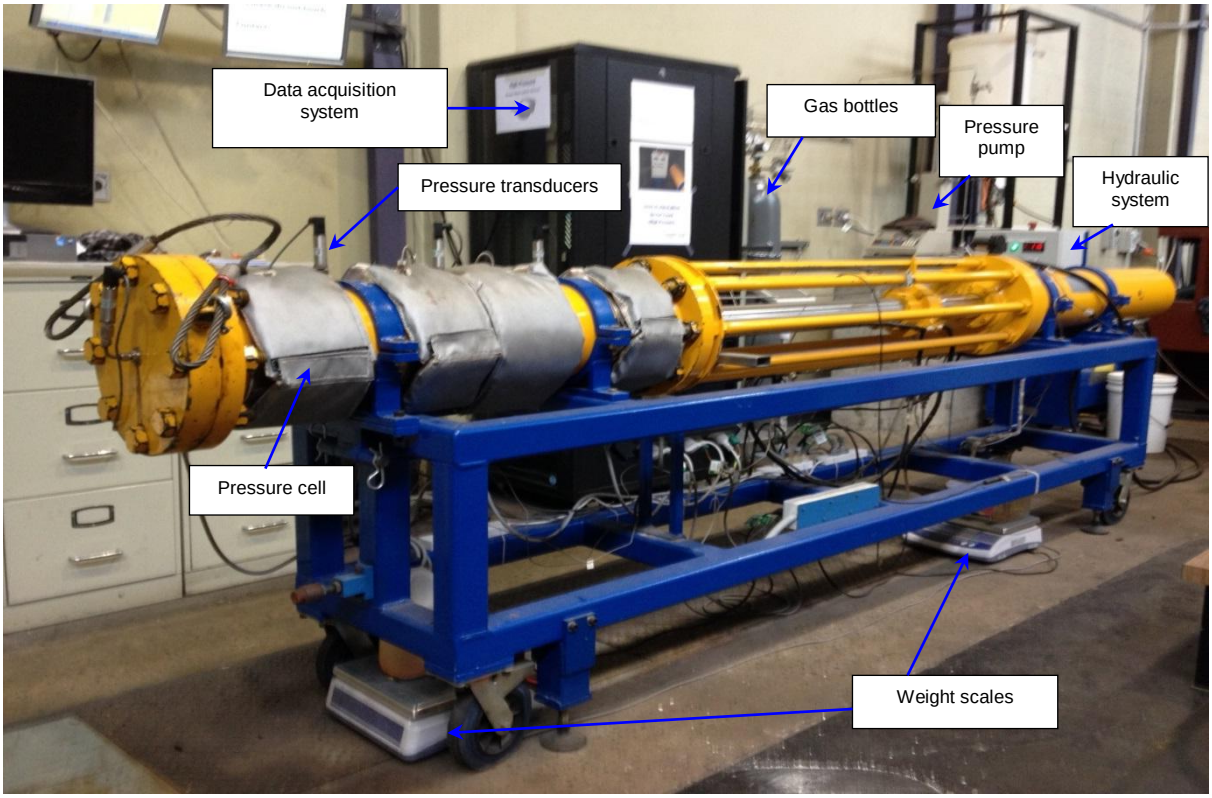

(b)

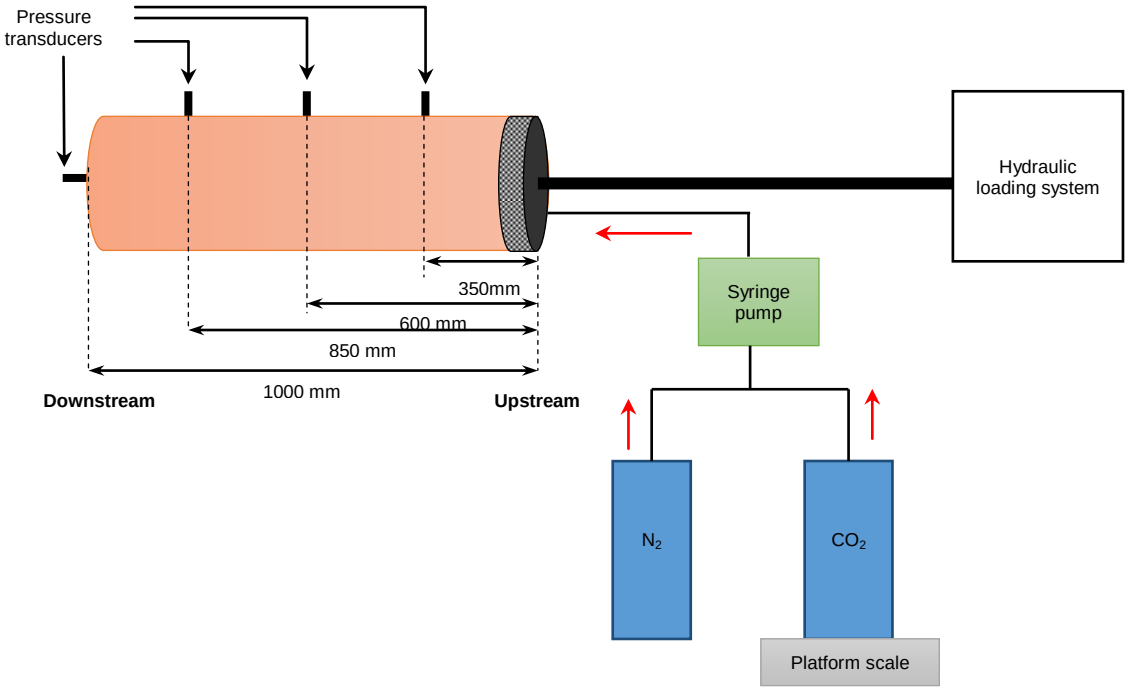

Fig 4. (a) Advanced core flooding apparatus (Ranathunga et al. 2015) and (b) the schematic diagram of the system

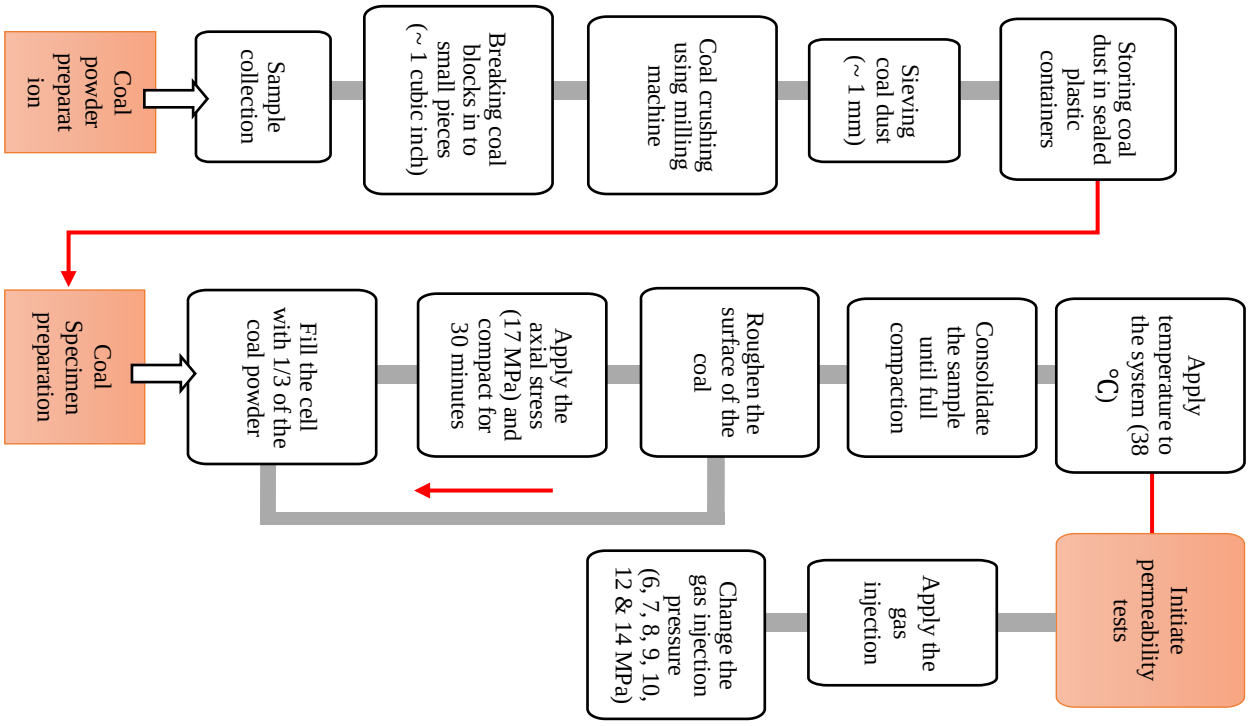

Fig 5. Experimental program for core flooding tests

2.2 Permeability tests

Permeability tests were conducted for CO_2 injections at seven different injecting pressures (6, 7, 8, 9, 10, 12 and 14 MPa) under 17 MPa axial stress, maintaining the system temperature at 38 ℃. Since the system temperature was maintained at 38 ℃, 6 and 7 MPa CO_2 injections were under sub-critical conditions and the rest of the CO_2 injections were under super-critical conditions (beyond 7.38 MPa pressure and 31.8^0C temperature CO_2 exists as a super-critical fluid). The undrained condition was maintained to determine the sample permeability, and the pressure-transient approach was used calculate the permeability (Pan et al. 2010; Perera et al. 2011). CO_2 injection was performed, maintaining the injection pressure at a steady state at each injection pressure (6, 7, 8, 9, 10, 12 and 14 MPa). The corresponding pressure developments at intermediate points along the sample and downstream were monitored and recorded using an advanced data acquisition system.

The permeability of the coal sample was then calculated using the pressure decay between the upstream and downstream vessels through the specimen calculated using Eqs. [1] and [2] (Pan et al. 2010; Wang et al. 2015):

$$\frac{(P_u - P_d)}{\Delta P_0} = e^{-\alpha t} \quad [1]$$

$$\alpha = \frac{kA}{\mu \beta L} V_s \left(\frac{1}{V_u} + \frac{1}{V_d}\right) \quad [2]$$

where, P_u is upstream vessel pressure, P_d is downstream vessel pressure, ΔP_0 is the step change of pressure in vessels at time = 0, t is time, k is permeability of the specimen, A is cross-section area of the sample (0.0324 m^2), L is the length of the sample (937 mm for this study after full consolidation), μ is the viscosity of the injecting fluid, β is the adiabatic compressibility of the injecting fluid, V_s is the sample volume, and V_u and V_d are the volume of upstream and downstream pressure vessels, respectively. The viscosity and the adiabatic compressibility were calculated using the REFPROP database (McLinden et al. 1998) for respective CO_2 pressures and a constant temperature (38 ℃). The pressure decay curves and corresponding permeability values of the sample for 17 MPa axial stress are shown in Fig. 6.

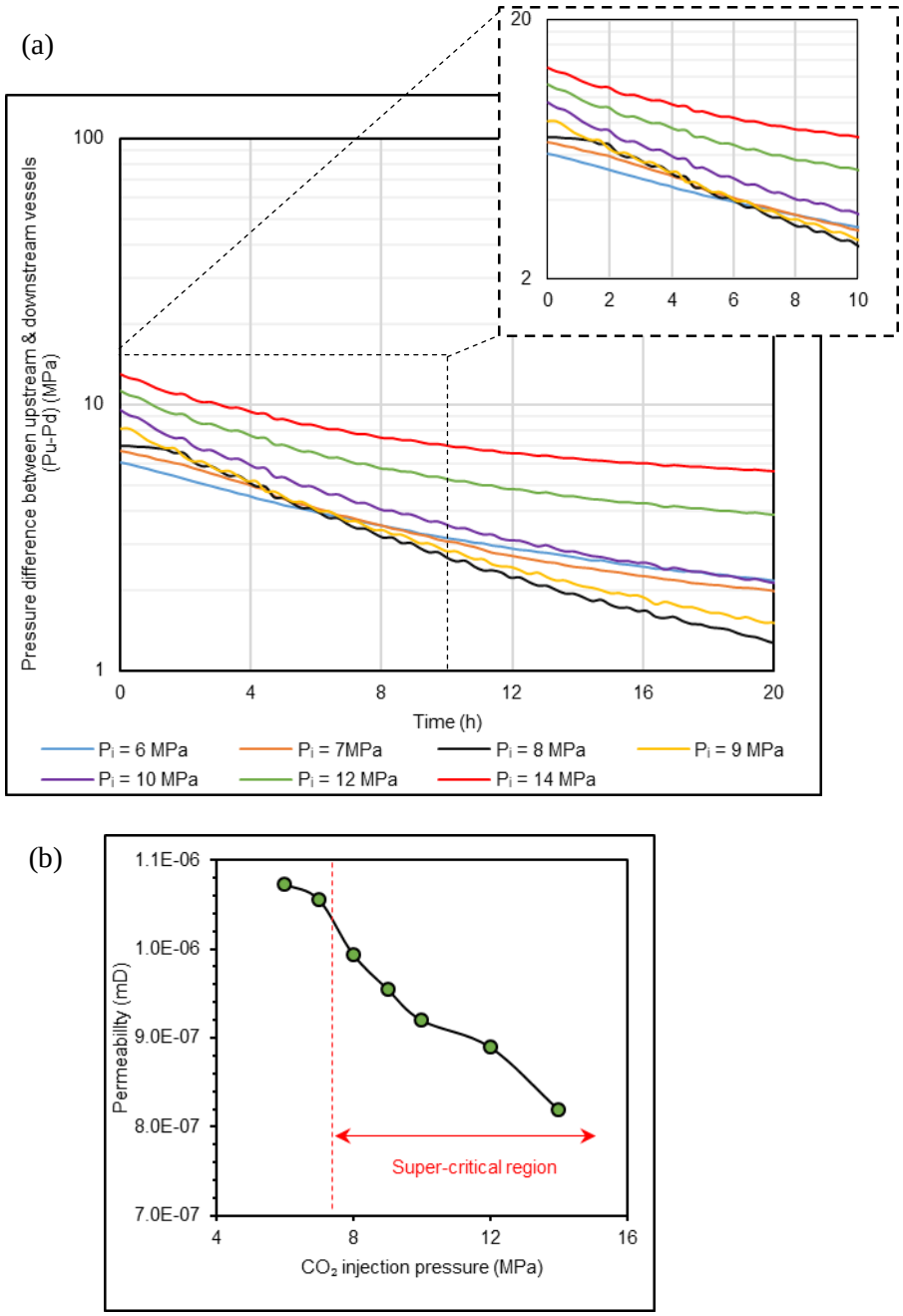

Fig 6. (a) Pressure decay curves (for 20 hours) and (b) CO_2 permeability variation with CO_2 injection pressures for 17 MPa axial stress

2.3 Coal matrix swelling measurements

During each test, the sample length variation was recorded using a linear variable differential transformer (LVDT) at 1s intervals to quantify the CO_2 adsorption-induced coal matrix swelling in the RC specimen. The volumetric swelling was then calculated using the measured length change of

the sample using Eq. [3], because movement in the radial direction was restrained in the tests by the steel casing. When the sample was subjected to swelling, the sample length was accordingly increased and for a shrinkage, the sample length was consequently decreased.

$$\text{Volumetric strain of the coal sample} = \frac{L_t - L_o}{L_o} \times 100\% \quad [3]$$

where, L_t is the sample length at time t and L_o is the sample length at time t = 0.

3 Results and discussion

A series of permeability tests was conducted for seven different CO_2 injection pressures under 17 MPa axial stress using a macro-scale RC low rank coal sample, and the results obtained are discussed in the following sections.

3.1 Carbon dioxide flow along the coal sample

3.1.1 Effect of injected carbon dioxide properties on coal mass permeability

According to Fig. 6(b), CO_2 permeability reduces with increasing CO_2 injection pressure at 17 MPa axial stress, and the reduction is relatively higher for super-critical CO_2. For example, increasing the injection pressure from 6 to 7 MPa sub-critical CO_2 flow caused around 11% permeability reduction and increasing the injection pressure from 8 to 9 MPa super-critical CO_2 flow caused a much larger permeability reduction of around 38%. As explained previously, CO_2 adsorption-induced coal matrix swelling is the main causative factor for this observed permeability reduction with increasing injection pressure. Similar results were reported by Ranathunga et al. (2015) for 11 MPa axial stress following similar macro-scale tests using the same type of RC coal samples, and a comparison of CO_2 permeability variations at 11 and 17 MPa axial stresses with respective to volumetric strain is presented in Fig. 7.

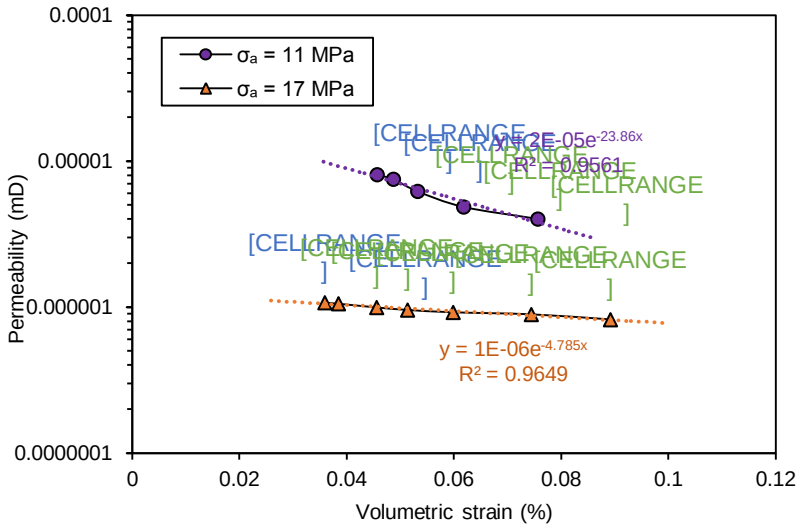

Fig 7. CO_2 permeability vs. coal mass volumetric strain variation under 11 MPa (Ranathunga et al. 2015) and 17 MPa axial stresses (Blue data labels denote sub-critical and green data labels denote super-critical CO_2 injections)

According to Fig. 7, CO_2 permeability and the volumetric swelling of the specimen follows a negative exponential variation at both axial stresses, confirming the reason for the observed reduced CO_2 flow-ability with injection pressure. According to Day et al. (2010), higher adsorption capacity of CO_2 at higher pressures results in greater matrix alterations, causing reduced permeabilities. Fig. 8 shows the variation of CO_2 properties of viscosity and compressibility with increasing CO_2 pressure at 38 ℃ (the temperature used for the current experiment). According to Fig. 8, CO_2 properties are significantly changed in the super-critical region, where significant increments in viscosity and reductions in compressibility with increasing pressure can be seen. This inordinate increment of viscosity (see Figs. 8(a) and (c)) provides higher fluidity for super-critical CO_2, which increases the adsorption capacity of the coal mass, and the reduction of compressibility of super-critical CO_2 (see Fig. 8(b)) constrains the amount of CO_2 molecules entering the coal matrix. These are the reasons for greater coal mass swelling and the lower permeabilities obtained with increasing CO_2 injection pressures.

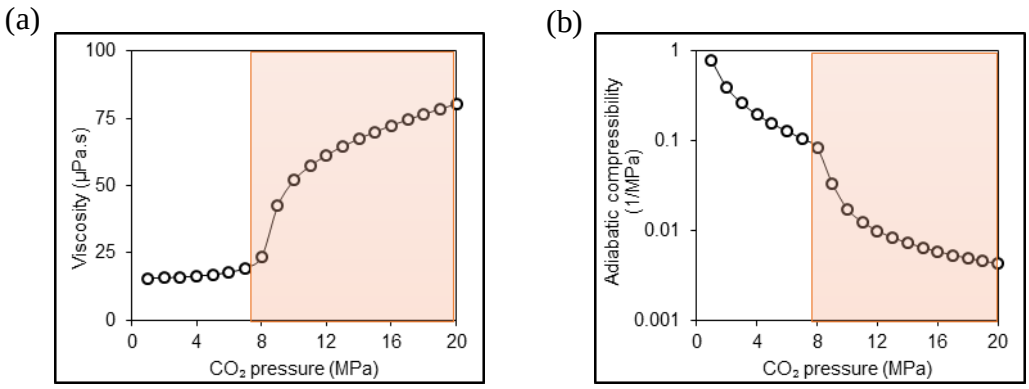

Fig 8. Variation of CO_2 properties (a) viscosity and (b) compressibility with pressure (McLinden et al. 1998) (The shaded area is under super-critical conditions)

3.1.2 Effect of coal seam depth on permeability

According to Fig. 7, a reduction of permeability from 11 to 17 MPa axial stress increment can be observed, similar to previous studies using small coal samples (Ranathunga et al. 2016; Vishal and Singh 2015). The disruptions to the flow with increased effective stresses cause these permeability decreases. However, the CO_2 flow reduction is comparatively less for super-critical CO_2 injection than for sub-critical CO_2. For example, a reduction of around 86% for 6 MPa sub-critical CO_2 injection and around 80% for 8 MPa super-critical CO_2 injection can be seen when the axial stress is increased from 11 to 17 MPa. Similar results were obtained by Ranathunga et al. (2016) for small coal samples of similar low rank coal and these researchers observed 82% and 77% decrease of permeability for 6 MPa (sub-critical) and 9 MPa (super-critical) CO_2 injections for 11 to 17 MPa confining pressure increase. This may be due to the already reduced flow with higher coal mass swelling and higher effective stress application in deeper coal seams that lead only to a lower reduction of super-critical CO_2 flow. This suggests that that, regardless of sample size, the effect of seam depth on its permeability is significant.

As discussed in Section 3.1.1, an increase of CO_2 injection pressure from 6 to 7 MPa (sub-critical flow) and 8 to 9 MPa (super-critical flow) cause a permeability reduction of 11 % and 38% respectively for 17 MPa axial stress. For similar CO_2 injection pressure increments during 11 MPa axial stress, Ranathunga et al. (2015) observed around 5% (6 to 7 MPa) and 23% (8 to 9 MPa)

permeability reductions for similar macro-scale RC samples made with the same brown coal. This implies that the permeability reduction with increasing injection pressure observed at 17 MPa axial stress is higher than the reduction observed at 11 MPa axial stress (Ranathunga et al. 2015). Similar results have been obtained for a meso-scale study by Ranathunga et al. (2016) for similar rank coal samples, which showed around 2% and 11% permeability reductions for 11 and 17 MPa confining pressures when CO_2 injection pressure was increased from 6 to 7 MPa, and 19% and 30% permeability reductions when CO_2 injection pressure was increased from 8 to 9 MPa at the same confining pressures (see Table 1). The reason is the lower flow ability at higher applied effective stresses, which offers a longer residential time for the CO_2 molecules within the coal mass. This may lead to higher matrix alterations causing lower permeability, especially for super-critical CO_2 flow (Vishal and Singh 2015).

The other important fact is that the coal matrix swelling is comparatively less at 17 MPa than for 11 MPa axial stress (see Fig. 7). For example, around 0.045% and 0.036% volumetric strains can be seen for 6 MPa (sub-critical) CO_2 flow and 0.053% and 0.046% for 8 MPa (super-critical) CO_2 flow under 11 MPa and 17 MPa axial stresses, respectively (see Fig. 7). This may be due to the obstruction of sample length variation by the higher stresses applying at higher axial stresses (recall Section 2.3). In addition, this volumetric strain increment with injection pressures is higher for 11 MPa axial stress compared to 17 MPa axial stress. For instance, a 6 to 7 MPa sub-critical CO_2 flow increment shows around 7.2% and 4% volumetric strain increases for 11 and 17 MPa axial stresses, while that for 8 to 9 MPa super-critical flow is around 16.1% and 12.6%, respectively (see Fig. 7). Similar results have been reported by Jasinge (2010) for RC low rank coal of a similar type. Jasinge (2010) observed around 8.9% and 3.8% swelling increments for 9 to 10 MPa confining pressure increments when CO_2 pressure was increased from 2.5 to 3.4 MPa. As explained previously, the higher effective stresses acting on the coal mass at greater axial stresses slow down the CO_2 flow along the coal matrix, offering less opportunity for CO_2 to interact with the coal mass by increasing the matrix rearrangements. Hol et al. (2011) also confirmed this

observation after finding a lower CO_2 sorption capacity for bituminous coal due to the higher in situ stresses applied on coal mass which will result in lesser matrix swelling. This shows the lower coal matrix swelling effect expected for CO_2 injection at greater seam depths. This is preferable for CO_2 sequestration as most of the potential seams for CO_2 sequestration process are at quite deep depths (> 1 km).

3.1.3 How does carbon dioxide flow behaviour vary along the seam?

As discussed in Sections 3.1.1 and 3.1.2, lower CO_2 injection pressures at shallow depths produce higher permeability through the coal mass, while higher CO_2 pressures at deeper depths cause flow reduction with enhanced coal matrix swelling and higher effective stresses applied on the coal mass. The meso-scale study conducted by Perera et al. (2011) for black coal (high rank), showed a considerable reduction in pressure along the coal mass during CO_2 injection. For example, around 6 MPa downstream pressure was observed for 10 MPa CO_2 injection under 15 MPa confinement and around 3 MPa for 20 MPa confinement for the same injection pressure. Similar lower pressure gradients were observed by Ranathunga et al. (2015) for a low rank macro-scale coal sample, and non-linear pressure variation along the specimen could be seen. Therefore, it was interesting to study how this CO_2 flow varies through the coal sample length (937 mm for the current study) during each injection conditions under this greater axial stress condition. Fig. 9 illustrates how the CO_2 pressure varied along the length of the sample during 6 MPa (sub-critical) and 8 MPa (super-critical) CO_2 injections at both 11 and 17 MPa axial stresses at the end of injection period measured using intermediate pressure transducers (see Fig. 4). The injection period was the duration of time taken to reach to the steady state at downstream and the additional 10 days (approximately) allowed for swelling-induced matrix changes.

As shown in Fig. 9, the respective injection pressures dropped gradually from upstream to downstream, regardless of injection pressure or depth (axial stress). The important thing is that this decrease is greater at higher injection pressures (super-critical) and higher depths compared to lower pressures and shallow depths. For example, 6 MPa sub-critical CO_2 flow under 11 MPa axial

stress caused a decrease of 21.4% from upstream to downstream, while the same injection under 17 MPa axial stress caused a greater reduction of 32.9%. In addition, 8 MPa super-critical CO_2 flow under 11 MPa axial stress produced a 29.8% drop in pressure, and 17 MPa axial stress caused a greater reduction of 43.6%. These lower pressure gradients caused lower permabilities through the sample (Fig. 7). Interestingly, the injected pressure remained constant up to around 500 m, 200 m, 400 m and 50 m during 6 MPa and 8 MPa CO_2 injection under 11 MPa and 17 MPa axial stress respectively. Nevertheless, this length reduced with increasing injection pressure and axial stress. Hence, it can be deduced that the critical zone of influence (area of CO_2 injection pressure kept constant) during CO_2 injection into a coal seam is larger at lower injection pressures at shallow depths, while it is reduced when higher CO_2 pressures are injected into deeper coal seams. This is important for the CO_2 storage process in deep coal seams.

Furthermore, only around 50% of the sample is under super-critical conditions under 11 MPa axial stress for 8 MPa CO_2 injection, and this proportion become less (around 25% of the sample) under 17 MPa axial stress (see Figs. 9(c) and (d)). This observation clearly indicates the lower volumetric strain increments at higher effective stresses (refer to Section 3.1.2). The reason is that the coal matrix alterations due to more adsorptive super-critical CO_2 occur over a smaller area of the sample due to the lower permeabilities at higher effective stresses. Hence, the volumetric strain increment is lesser at greater depths than shallow depths.

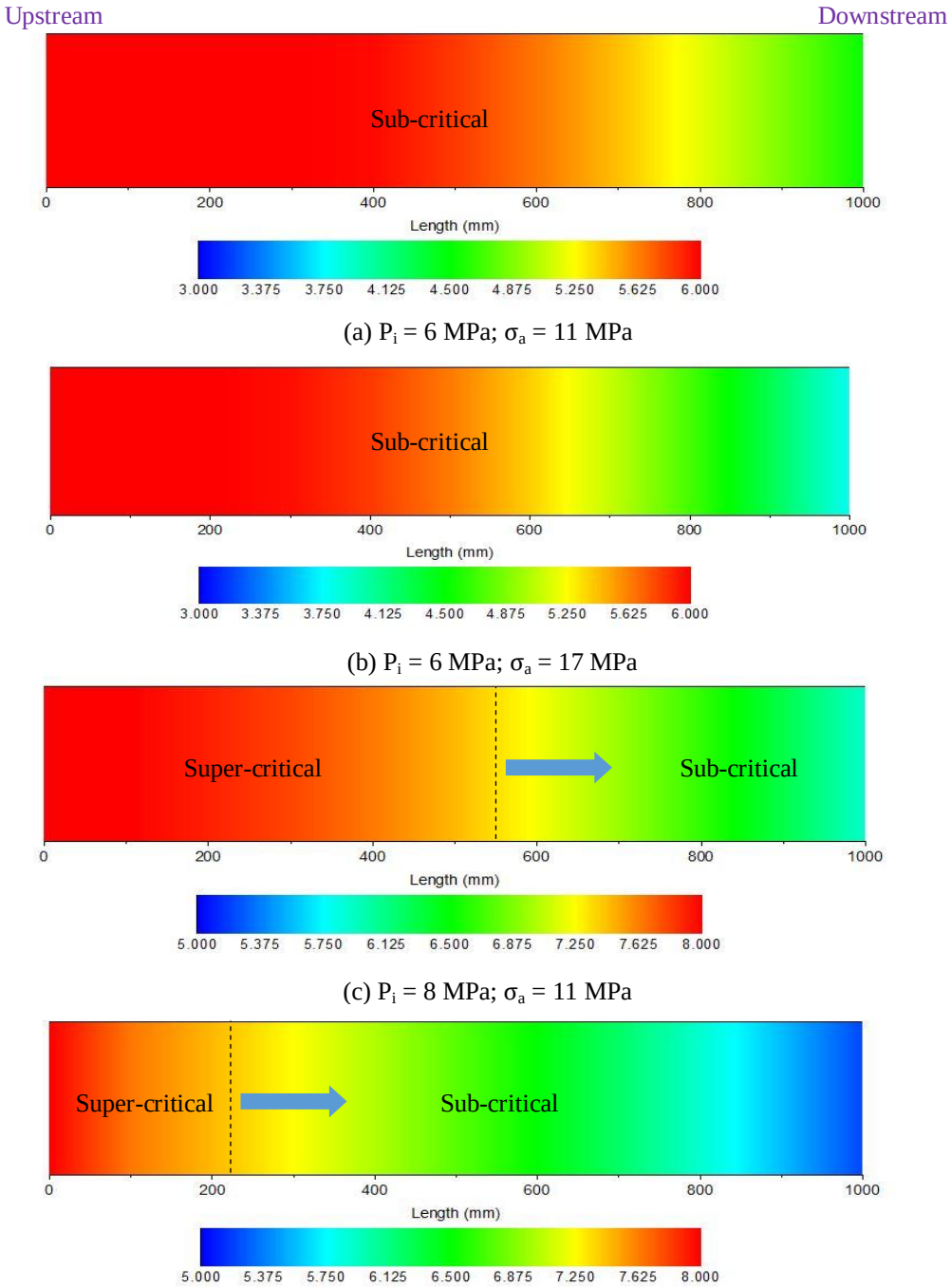

(a) P_i = 6 MPa; σ_a = 11 MPa

(b) P_i = 6 MPa; σ_a = 17 MPa

(c) P_i = 8 MPa; σ_a = 11 MPa

(d) P_i = 8 MPa; σ_a = 17 MPa

Fig 9. Pressure variation along the length of the sample after injection period under 11 MPa (Ranathunga et al. 2015) and 17 MPa axial stresses (Here, P_i is injection pressure and σ_a is axial stress. The colour scale of each figure depicts the CO_2 pressure (in MPa) variation along the coal sample)

3.1.4 *An empirical relationship for carbon dioxide flow variation along a low rank coal seam*

As CO_2 permeability along the coal sample varies with both axial stress and CO_2 injection pressure, a multi-variable regression equation was developed for permeability variations using the experimental data from Ranathunga et al. (2015) and the present study. Refer to Eq. [4]:

$$k = e^{(-0.2944\sigma_a - 0.1105P_i - 7.9127)} \qquad R^2 = 0.936 \qquad [4]$$

where, σ_a is axial stress (MPa), P_i is CO_2 injection pressure (MPa) and k is CO_2 permeability (mD). The predicted permeability variations with the axial stresses and CO_2 injection pressures are shown in Fig. 10. Fig. 10 clearly indicates that CO_2 permeability is higher at lower axial stresses and lower CO_2 injection pressures. In addition, it is reduced gradually with the increment of both axial stress and CO_2 injection pressure, confirming the experimental observations.

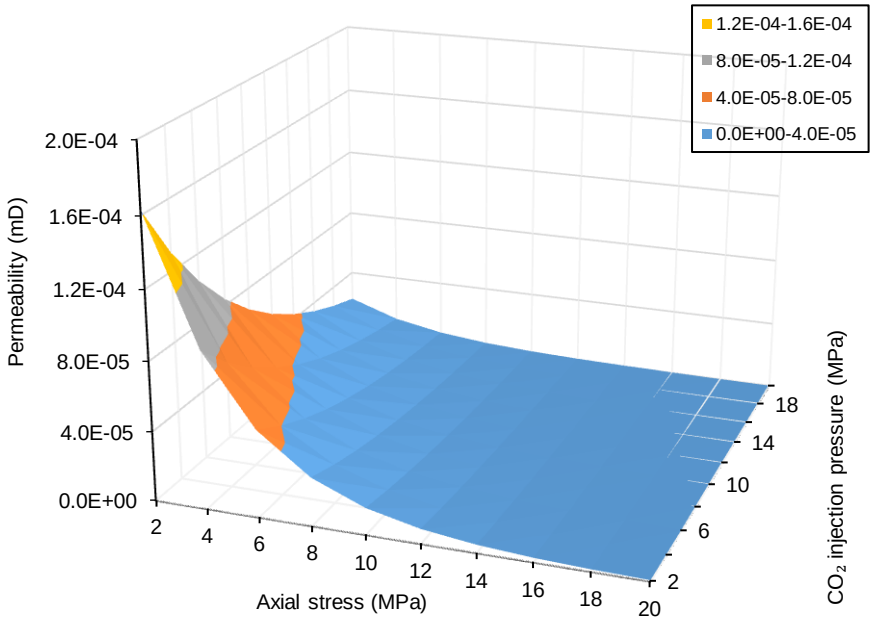

Fig 10. Predicted permeability variation with axial stress and CO_2 injection pressure

3.2 CO_2 storage capacity variation

One of the main purposes of CO_2-ECBM process is to store anthropogenic CO_2 in deep un-mineable coal seams. It is therefore vital to investigate the amount of CO_2 that can be stored in the coal mass under various conditions, including various seam depths (axial stress) and injecting fluid properties (CO_2 phase and pressure). The next stage of analysis was therefore to quantify the CO_2

storage capacity in the coal mass under the various test conditions. This was accurately monitored using a digital platform scale at the CO_2 injection point. The amount of gas injected was monitored over time after changing the injection pressure and maintaining it for more than 10 days, to allow sufficient time for swelling. Fig. 11 shows the variation in amount of injected CO_2 into the coal mass (after around 10 hours) with effective stress under 11 MPa and 17 MPa axial stress conditions at each injection pressure. The effective stress was calculated as the difference between the applied axial stress and the mean gas pressure (the average of the pressures applied at upstream and downstream).

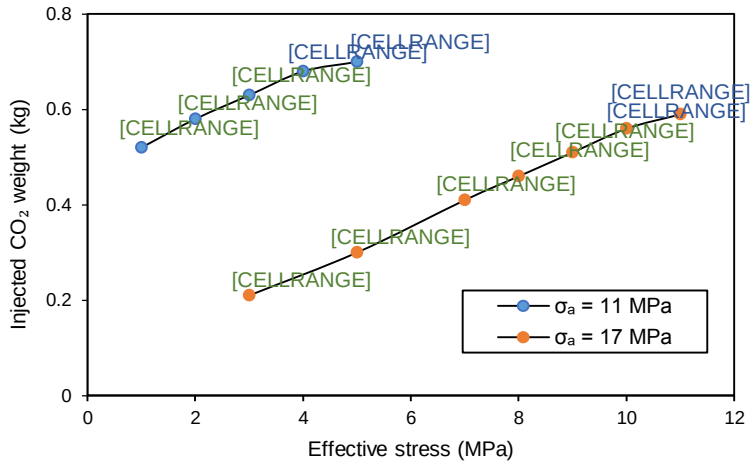

Fig 11. Variation of injected CO_2 weight (after 10 days) and CO_2 permeability with effective stress for 11 and 17 MPa axial stresses (The blue data labels denote the sub-critical and the green data labels denote the super-critical CO_2 injections).

According to Fig. 11, the amount of injected CO_2 is increased with increasing effective stress for both 11 and 17 MPa axial stresses. This increment is greater when the CO_2 injection pressure is greater than 7 MPa (super-critical flow) and lower for 6 to 7 MPa (sub-critical flow) CO_2 injections. For example, around 4.9% increment in injected CO_2 weight was observed from 6 to 7 MPa pressure increment, and that for 8 to 9 MPa was 14.9% at 11 MPa axial stress. Similarly, for 17 MPa axial stress, the injected CO_2 weight was around 1.9% for an increase from 6 to 7 MPa pressure and 9.8% for 8 to 9 MPa pressure increment. The main reason for this observation is the reduction of CO_2 flow with increasing injection pressure (see Fig. 7) due to the coal matrix

rearrangements which require less CO_2 injection into the coal sample. Furthermore, the higher the axial stress, the greater the effective stress application, which causes greater reductions in CO_2 injectivity (see Fig. 10).

However, this CO_2 storage process is time-dependent, and longer time offers more opportunity for CO_2 adsorption and storage. Fig.12 shows the injected CO_2 weight variation with time at 6 MPa (sub-critical) and 8 MPa (super-critical) injection pressures under both 11 and 17 MPa axial stresses. According to Fig. 12, the cumulative weight of injected CO_2 increases over time, and the rate of increase is lower at higher CO_2 injection pressures and at greater axial stresses. For example, the average increases are around 0.0031 and 0.0025 at 6 and 8 MPa CO_2 injection pressures under 11 MPa axial stress, while they are around 0.0008 and 0.0005 for the same injection pressures (6 and 8 MPa) under 17 MPa axial stress. This observation clearly explains the CO_2 storage behaviour observed in Fig. 11, which shows greater CO_2 storage capacity at lower depths and lower CO_2 injection pressures.

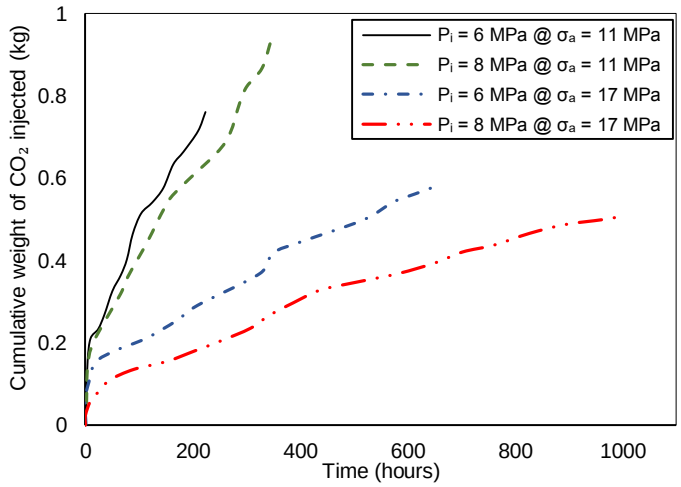

Fig 12. Cumulative weight of injected CO_2 variation with time for 6 MPa and 8 MPa injection pressures at 11 MPa and 17 MPa axial stresses

Interestingly, in relation to the weight of CO_2 injected at the end of the injection period, a contrasting behaviour compared to that shown in Fig. 11 was obtained. Fig. 13 illustrates a comparison of the weight of CO_2 injected after 10 days of injection and at the end of the injection

period under both 11 and 17 MPa axial stresses. According to Fig. 13, it can be noted that, although flow ability reduces at higher CO_2 injection pressures, a comparatively larger amount of CO_2 can be stored if a long time is offered for CO_2 sequestration at greater depths. The reason is, as stated in Fig. 8, the inherent liquid-like properties of super-critical CO_2 permit greater adsorption potential with the coal matrix, which requires some time to complete.

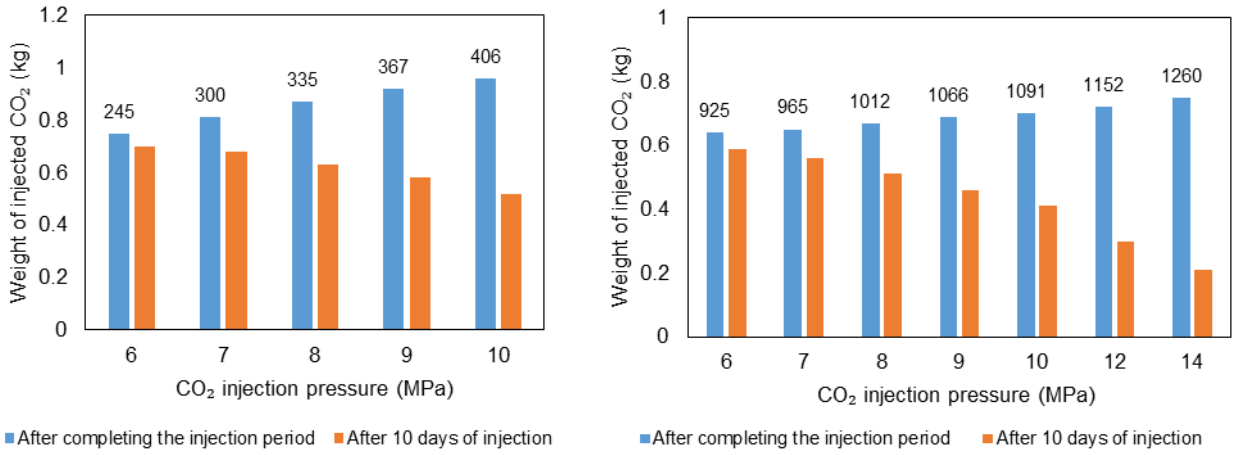

Fig 13. Comparison of weight of CO_2 injected after completing the injection period and after 10 days during (a) 11 MPa axial stress and (b) 17 MPa axial stress (The data labels denote the injection period (in hours) for each injection pressure)

However, in the case of CO_2 storage capacity variation with axial stress, the injected CO_2 weight reduction with axial stress is not much lower compared to the permeability reduction observed with axial stress (see Fig. 7). A comparison of the observed permeability reductions and the CO_2 storage capacity reductions under 11 to 17 MPa axial stress increment is shown in Table 2.

Table 2. Comparison of permeability and CO_2 injectivity reductions with 11 MPa to 17 MPa axial stresses

	CO_2 injection pressure (MPa)	Permeability reduction (%)	Injected CO_2 weight reduction (%)
Sub-critical region	6	86.72	27.08
	7	85.96	25.01
Super-critical region	8	83.98	22.99
	9	80.31	19.75
	10	77.06	14.67

According to Table 2, similar to permeability reduction, the injected CO_2 or stored CO_2 weight is greatly reduced in the super-critical region, and the permeability reduction is around 60~70% higher than the injected CO_2 weight reductions (see Table 2). The higher residential time for CO_2 molecules with higher effective stresses may offer greater adsorption possibility for CO_2 molecules with the coal matrix (De Silva 2013) with time and the inceraesd amount of CO_2 molecules enter to the coal mass at higher CO_2 pressures, warranting lower reductions than in flow ability.

4 Suggestions for CO_2-ECBM field applications

Potential coal seams for CO_2-ECBM are located deep underground, where the injected CO_2 is in its super-critical state (beyond 7.38 MPa and 31.8 ℃). The liquid-like viscosities (see Fig. 8) of super-critical CO_2 provide more potential for stable CO_2 storage within the coal matrix. Nevertheless, the observed decrease in CO_2 flow ability along the coal matrix, especially during super-critical CO_2 injection, raises concerns concerning the productivity of the ECBM process. On the other hand, according to the findings, regardless of the permeability reductions, CO_2 storage capacity in coal increases with increasing injection pressure upon offering sufficient time for sequestration. Furthermore, a comparatively lower reduction of CO_2 storage capacity was witnessed with increasing axial stress from 11 MPa (representing an approximately 400 m deep coal seam) to 17 MPa (representing an approximately 600 m deep coal seam). This information is very useful for CO_2 sequestration field projects, because there is current interest in utilising extremely deep underground coal seams for CO_2 sequestration. According to current findings, this depth effect does not have such a great influence on CO_2 storage potential.

However, attention should be paid to the flow reductions which occur with the coal matrix swelling, because this might affect long-term CO_2 sequestration processes by allowing more CO_2

adsorption, which has been witnessed in several field-scale projects (White et al. 2005). Therefore, the implementation of flow-enhancement techniques (e.g. hydro fracturing, alternative injection of N_2) (White et al. 2005) will provide more opportunities to store greater amounts of CO_2 in deeper coal seams.

Hence, resolving complications when using super-critical CO_2 for CO_2-ECBM recovery in terms of CO_2 storage capacity and CH_4 production enhancement using flow-enhancement techniques is essential prior to field-scale projects.

5 Conclusions

Following a series of CO_2 permeability tests using macro-scale low rank coal specimens, the following conclusions can be drawn:

- CO_2 permeability in coal is greater at lower depths and lower CO_2 injection pressures, while it gradually reduces with increasing depth and injection pressure, and the associated effective stress variation and the coal matrix swelling caused by CO_2 adsorption are the main causative factors, respectively.
- Super-critical CO_2 causes greater swelling in the coal mass compared to sub-critical CO_2, and the swelling increases with increasing injection pressure, regardless of depth. This swelling increment is however reduced with increasing seam depth, probably due to the associated greater effective stresses effect that obstructs CO_2 flow along the coal matrix, offering less opportunity for CO_2 to interact with the coal mass.
- The permeability variation along the coal sample under the tested coal seam and injecting CO_2 conditions can be effectively represented using a simple multivariable regression model, and such models play an important role in field projects to predict CO_2 flow migration along the seam.
- The observed CO_2 permeability along the tested coal specimen indicated that the critical zone of influence for CO_2 injection into a selected coal seam is greater at lower injection pressures and at shallow depths, and it this reduces with increasing CO_2 pressure and seam depth.

- Finally, the observed CO_2 storage capacity of the tested coal under various conditions revealed that CO_2 storage capacity in a coal seam is greater at lower depths and higher CO_2 injection pressures. However, the reduction of CO_2 storage capacity with depth was not significant, which is important for field CO_2 sequestration projects, which normally use deep seams to store CO_2.

Acknowledgements

The authors wish to express their appreciation for the funding provided by the Australian Research Council (DE130100124).

References

Day S, Fry R, Sakurovs R (2008) Swelling of Australian coals in supercritical CO_2. International Journal of Coal Geology 74:41-52

De Silva PNK (2013) A study of CO_2 storage capacity in sedimentary rocks. PhD dissertation, Monash University, Melbourne, Australia.

Hol S, Spiers CJ (2012) Competition between adsorption-induced swelling and elastic compression of coal at CO_2 pressures up to 100MPa. Journal of the Mechanics and Physics of Solids 60:1862-1882

Jasinge D (2010) An investigation of the effect of carbon dioxide sequestration on the behaviour of brown coal. PhD dissertation, Monash University, Melbourne, Australia.

Xie J, Gao M, Yu B, Zhang R, Jin W (2015) Coal permeability model on the effect of gas extraction within effective influence zone. Geomechanics and Geophysics for Geo-Energy and Geo-Resources 1:15-27

Larsen JW, Flowers RA, Hall PJ, Carlson G (1997) Structural rearrangement of strained coals. Energ Fuel 11:998-1002

530 Liu Q, Cheng Y, Ren T, Jing H, Tu Q, Dong J (2016) Experimental observations of matrix swelling
531 area propagation on permeability evolution using natural and reconstituted samples. Journal
532 of Natural Gas Science and Engineering 34:680-688
533 Masoudian MS, Airey DW, El-Zein A, (2014) Experimental investigations on the effect of CO_2 on
534 mechanics of coal. International Journal of Coal Geology 128:12-23
535 McLinden M, Klein S, Lemmon E, Peskin A (1998) REFPROP, Thermodynamic and transport
536 properties of refrigerants and refrigerant mixtures. NIST Standard Reference Database 23,
537 Gaithersburg, MD.
538 Merkel A, Gensterblum Y, Krooss BM, Amann A (2015) Competitive sorption of CH_4, CO_2 and
539 H_2O on natural coals of different rank. International Journal of Coal Geology 150–151:181-
540 192
541 Pan Z, Connell LD (2007) A theoretical model for gas adsorption-induced coal swelling.
542 International Journal of Coal Geology 69:243-252
543 Pan Z, Connell LD, Camilleri M (2010) Laboratory characterisation of coal reservoir permeability
544 for primary and enhanced coalbed methane recovery. International Journal of Coal Geology
545 82:252-261
546 Perera MSA, Ranjith PG, Airey DW, Choi SK (2011) Sub- and super-critical carbon dioxide flow
547 behavior in naturally fractured black coal: An experimental study. Fuel 90:3390-3397
548 Ranathunga AS, Perera MSA, Ranjith PG, Ju Y, Vishal V, De Silva PNK (2015) A macro-scale
549 experimental study of sub-and super-critical CO_2 flow behaviour in Victorian brown coal.
550 Fuel 158:864-873
551 Ranathunga AS, Perera MSA, Ranjith PG (2016) Super-critical carbon dioxide flow behaviour in
552 low rank coal: A meso-scale experimental study. Journal of CO_2 Utilization (under review)
553 Sun Y, Li Q, Yang D, Liu X (2016) Laboratory core flooding experimental systems for CO_2
554 geosequestration: An updated review over the past decade. Journal of Rock Mechanics and
555 Geotechnical Engineering 8:113-126

556 Siriwardane H, Haljasmaa I, McLendon R, Irdi G, Soong Y, Bromhal G (2009) Influence of carbon
557 dioxide on coal permeability determined by pressure transient methods. International
558 Journal of Coal Geology 77:109-118.
559 Verma AK, Sirvaiya A (2016) Comparative analysis of intelligent models for prediction of
560 Langmuir constants for CO_2 adsorption of Gondwana coals in India. Geomechanics and
561 Geophysics for Geo-Energy and Geo-Resources 2:97-109
562 Vishal V, Singh TN (2015) A Laboratory Investigation of Permeability of Coal to Supercritical
563 CO_2. Geotechnical and Geological Engineering 33:1009-1016
564 Wang S, Elsworth D, Liu J (2013) Permeability evolution during progressive deformation of intact
565 coal and implications for instability in underground coal seams. International Journal of Rock
566 Mechanics and Mining Sciences 58:34-45
567 Wang Y, Liu S, Elsworth D (2015) Laboratory investigations of gas flow behaviors in tight
568 anthracite and evaluation of different pulse-decay methods on permeability estimation.
569 International Journal of Coal Geology 149:118-128
570 White CM, Smith DH, Jones KL, Goodman AL, Jikich SA, LaCount RB, DuBose SB, Ozdemir E,
571 Morsi BI, Schroeder KT (2005) Sequestration of Carbon Dioxide in Coal with Enhanced
572 Coalbed Methane Recovery: A Review. Energy and Fuels 19:659-724